



Delft University of Technology

## np-CECADA

### Enhancing Ubiquitous Connectivity of LoRa Networks

Kouvelas, Nikolaos; Venkatesha Prasad, R.; Yazdani, Niloofar; Lucani, Daniel E.

#### DOI

[10.1109/MASS52906.2021.00054](https://doi.org/10.1109/MASS52906.2021.00054)

#### Publication date

2021

#### Document Version

Final published version

#### Published in

2021 IEEE 18th International Conference on Mobile Ad Hoc and Smart Systems (MASS)

#### Citation (APA)

Kouvelas, N., Venkatesha Prasad, R., Yazdani, N., & Lucani, D. E. (2021). np-CECADA: Enhancing Ubiquitous Connectivity of LoRa Networks. In C. Ceballos (Ed.), *2021 IEEE 18th International Conference on Mobile Ad Hoc and Smart Systems (MASS): Proceedings* (pp. 374-382). Article 9637758 IEEE. <https://doi.org/10.1109/MASS52906.2021.00054>

#### Important note

To cite this publication, please use the final published version (if applicable).  
Please check the document version above.

#### Copyright

Other than for strictly personal use, it is not permitted to download, forward or distribute the text or part of it, without the consent of the author(s) and/or copyright holder(s), unless the work is under an open content license such as Creative Commons.

#### Takedown policy

Please contact us and provide details if you believe this document breaches copyrights.  
We will remove access to the work immediately and investigate your claim.

***Green Open Access added to TU Delft Institutional Repository***

***'You share, we take care!' - Taverne project***

**<https://www.openaccess.nl/en/you-share-we-take-care>**

Otherwise as indicated in the copyright section: the publisher is the copyright holder of this work and the author uses the Dutch legislation to make this work public.

# *np*-CECADA: Enhancing Ubiquitous Connectivity of LoRa Networks

Nikolaos Kouvelas\*, R Venkatesha Prasad\*, Niloofar Yazdani<sup>\*‡</sup>, Daniel E. Lucani<sup>‡</sup>

\*Embedded and Networked Systems, TU Delft, <sup>‡</sup>DIGIT and Electrical and Computer Engineering, Aarhus University

**Abstract**—Long Range Wide Area Networks (LoRaWAN) offer ubiquitous communications for The Internet of Things (IoT). However, there are many challenges in rolling out LoRaWAN – mainly scalability, energy efficiency, Packet Reception Ratio (PRR), and keeping the channel access as simple as unslotted ALOHA. To this end, we design non-persistent Capture Effect Channel Activity Detection Algorithm (*np*-CECADA), which is a novel, distributed protocol for the MAC layer of LoRaWAN. It utilizes Channel Activity Detection (CAD), which is a built-in imperfect mechanism for channel sensing and minimal feedback from the gateways. In *np*-CECADA each device independently adapts backoff times based on the traffic in its vicinity and the transmission power based on the heuristically inferred probability of capturing the channel. To achieve this, first, we carried out an extensive on-field evaluation to measure the effectiveness of CAD and capture effect in LoRa. Using them we designed *np*-CECADA and developed *ns-3* modules. Packet Reception Ratio of *np*-CECADA is 15.74× and 5.13× higher than vanilla LoRaWAN and *p*-CARMA, respectively. Channel utilization is 11.24× higher compared to LMAC. Further, on a testbed of 30 LoRa devices *np*-CECADA outperforms LoRaWAN up to 5 times.

## I. INTRODUCTION

Among several Low Power Wide Area Network (LPWAN) technologies, Long Range (LoRa) WAN has been the most promising in offering an easily accessible, deployable, and almost no maintenance network [1]. The PHY layer of LoRa is a proprietary Chirp Spread Spectrum (CSS) communication technology that is robust against noise and multi-path fading [2], [3]. The LoRa-based network, LoRaWAN, is an open standard by the LoRa-Alliance. As seen in Fig. 1, LoRaWAN defines a star topology between end-devices and gateways, with asynchronous, bidirectional, AES-encrypted communication among them, allowing mostly uplink, i.e., transmissions from devices to gateways in their vicinity that forward the frames to a network server. Further, LoRa networks operate in ISM bands so they do not incur spectrum costs, but should coexist with other ISM network technologies and thus adhere to 1% duty cycle in data-transmission (frequency band of operation and regulation depend on the respective countries). We focus on *Class A* LoRaWAN since it is highly constrained. In *Class A* only two receiving windows are allowed per end-device after each transmission for downlink from the gateway. Several configurable parameters –such as, transmission power, carrier frequency, Coding Rate (CR), Spreading Factors (SF), channel bandwidth, and forward error correction– enable devices to trade-off data-rate, which can reach 50 kbps, for communication range, spanning from 5 km to 20 km depending on the area (dense urban to rural) [3], [4]. For detailed information regarding LoRa(WAN), refer to [5]. It is claimed, however, that unlicensed-band LPWANs like LoRaWAN cannot guarantee ubiquitous connectivity to cover the increasing pervasiveness

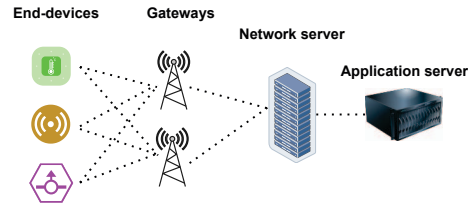


Fig. 1. LoRa Network.

of modern IoT applications[6]. The limitations are found in terms of capacity, described as the network throughput over its coverage area, and coexistence with other networks operating in the unlicensed spectrum.

In this paper, we address the capacity limitation of LoRa networks. Current vanilla-LoRaWAN cannot serve but only a few hundred IoT devices connected per gateway [7], mainly due to its unslotted Aloha type MAC, which we refer to as LoRaMAC hereafter. In particular, end devices broadcast any generated data frames immediately to the gateways in their vicinity regardless of the presence of any ongoing transmission [5]. This limits the theoretical maximum normalized throughput of a saturated LoRaWAN to 0.18 [8]. Since LoRaWAN is asynchronous in communication, favoring uplink, time-division approaches cannot be used to regulate the transmissions. Thus to accommodate higher traffic, more advanced solutions are needed in the MAC layer, incorporating observations from the PHY layer (LoRa), and leveraging Capture Effect (CE) and Channel Activity Detection (CAD).

**Capture Effect (CE).** CE defines the successful reception of a frame-transmission against its adversaries either due to its relatively higher Received Signal Strength (RSS) and/or due to having initiated its reception slightly earlier (i.e., time capture) [9]. Bor *et al.* and Fernandez *et al.* showed that the probability of frame-loss changes even with slight differences in RSS and/or transmission delay, thus necessitating a detailed investigation into the impact of CE in finding the capacity of LoRaWAN [7], [10]. In this work, we aim to increase the capacity of LoRaWAN by incorporating our on-field observations on CE. Thus, we consider extensive collision scenarios involving multiple LoRa-devices. By observing the frame reception when interferers of different powers and delay-offsets are involved, we define probabilistic rules under which frames are correctly received. By employing such rules in the MAC, the devices can adapt their transmission power to increase their success rate while at the same time avoid collisions. In LoRa-channels the effect of multi-path fading is intensified due to the high range of operation, increasing frame corruption/loss [11]. By adapting transmission power, devices can reduce the overall fading in LoRa-channels, and

thus improve the overall frame reception.

**Channel Activity Detection (CAD).** CAD is an optional functionality of LoRaWAN –somewhat similar to Carrier Sensing (CS)– wherein transmissions can be detected using cross-correlation with chirp-signals [12]. This makes CAD a candidate mechanism for the application of Carrier Sensing Multiple Access (CSMA) in LoRaWAN. CSMA techniques increase channel utilization and Packet Reception Ratio (PRR) and are widely utilized in wireless networks [8], [13]. However, incorporating CSMA in LoRa-devices is highly challenging. The reasons are: (i) Classic CSMA utilizes frequent feedback in the form of ACK messages. However, the LoRaWAN with *Class A* devices allows almost no feedback from gateways, precluding acknowledgments and Automatic Repeat reQuests (ARQ). (ii) LoRa-devices cannot sense the channel continuously due to their energy constraints. (iii) The higher communication range (in km) between devices and gateways also leads to the creation of many hidden devices [8]. (iv) Most importantly, LoRa-receivers can demodulate signals below the noise floor, hindering any reliable RSS-indication of channel occupancy that is used by CSMA [14]. (v) Due to the imperfections in CAD and the pseudo-orthogonality of SFs, concurrent multi-SF transmissions impair sensing and introduce false detections [14]. Although CAD is not a sophisticated CS-mechanism and was *not* designed for the CS as introduced in the literature [8], it could be leveraged to implement CSMA to evade collisions and increase network throughput in LoRaWAN [15], [14].

**Contributions.** Fig. 2 shows the potential gap between Classic *np*-CSMA and without CSMA. The addition of a naive Binary Exponential Backoff (BEB) mechanism [13] i.e., naive *np*-CSMA (blue line), increases, even more, the PRR achieved by serving a certain number of devices. For example, by applying naive *np*-CSMA the PRR increases from 2.6% to 35.6% for 3000 IoT devices, compared to vanilla LoRaMAC. Despite this huge gain, applying more sophisticated distributed algorithms will further improve the capacity of LoRaWAN. We design non persistent-Capture Effect, Channel Activity Detection Algorithm (*np*-CECADA), which raises the capacity of LoRaWAN while being energy efficient. Specifically, we get higher PRR as the number of LoRa-devices increases by avoiding frame collisions using the principles of *np*-CSMA in a LoRa network with significantly low feedback and several hidden devices. With *np*-CECADA, LoRa-devices: (i) utilize CAD not only to assess medium-occupancy but also to estimate the traffic in their vicinity and thus adapt their backoff value before attempting to transmit, and (ii) leverage CE-probabilities to adapt their transmission power– saving energy and reducing collisions. Note that the overhead due to *np*-CECADA is lower than classic *np*-CSMA, as our algorithm utilizes only the very rare downlink channels by the gateways and does not make use of RTS/CTS and ACKs. Further, vanilla LoRaMAC consumes more energy as it transmits all generated frames. Our contributions are multifold: 1) First we evaluate the CE in LoRa with respect to both power differences and delay offsets by conducting ex-

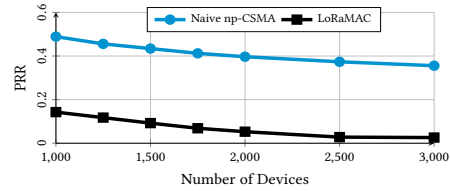


**Fig. 2. PRR: Naive *np*-CSMA (BEB) and vanilla LoRaWAN. 20 B frames on SF10, with 1% duty cycle.**

tensive on-field experiments to define the probabilities of successful transmissions (see § III-A).

- 2) We evaluate the performance and the limitations of the current LoRa chips (SX1261) in terms of CAD by conducting extensive on-field experiments (see § III-B).
- 3) We design *np*-CECADA, an adaptive, distributed, backoff time-based CS MAC protocol for LoRaWAN that can be employed on current LoRa-deployments *without* requiring any adaptation in the infrastructure (see subsection III-C).
- 4) We designed model of *np*-CECADA in *ns-3*. The CAD and CE modules in *ns-3* incorporate the results discovered in our on-field experiments in order to represent closest-to-reality simulations. We compare *np*-CECADA not only with classic LoRa implementation but also with the state-of-the-art algorithms in the MAC layer of LoRaWAN [14], [15] proving its superiority using many metrics (see § IV).
- 5) We employed *np*-CECADA in our LoRa testbed with 30 devices. To compare at scale, we increased the offered load correspondingly (see § V).

## II. RELATED WORK

Kleinrock and Tobagy proposed two variants of CSMA [8]: (a) persistent CSMA (*p*-CSMA) in which the medium is sensed continuously and transmits with probability  $p$  when it finds the medium idle. In case  $p = 1$  the transmission is unconditional, i.e., 1-CSMA. (b) non-persistent in which the device backs off for random duration when the medium is occupied and senses again, and finally transmits when the medium is assessed as free.

**MAC protocols for LoRaWAN.** Most of the approaches not involving CSMA are variants of time-scheduling. Polonelli *et al.* introduce a slotted Aloha variant on top of the pre-existing LoRaMAC, wherein devices use timestamps for the synchronization of transmissions [16]. In FREE each device buffers its data frames and transmits them in bulk to the gateway, which divides transmission time per channel, and schedules the same SFs sequentially and different SFs simultaneously [17]. S-MAC perceives the clock-drifts of periodic transmitters and groups the maximum number of collision-free and concurrent transmissions per SF at the same channel [18]. In TS-LoRa the time-slots are assigned by a hash algorithm that uses the frame-lengths to map the ID of each device into a unique time-slot [19]. In hybrid approaches, a part of the communication is time or frequency scheduled, and another part is based on Aloha [20], [21]. In RS-LoRa the gateway schedules devices in equally divided transmission frames per channel and subframes per SF. Then, the medium-access in subframes takes place in Aloha-fashion [20]. In RT-LoRa

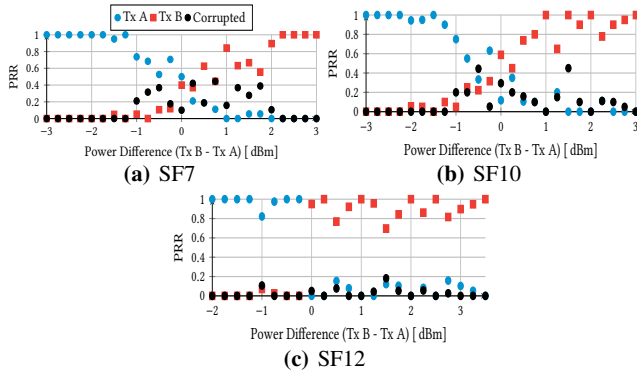


**Fig. 3. Effect of power on CE – two transmitters.**

non-periodic devices transmit in contention timeslots using slotted Aloha, and periodic devices transmit in contention-free timeslots using TDMA based on three different Quality of Service (QoS) classes [21].

**CSMA mechanisms.** Pham first investigated the utilization of CAD in CSMA approaches for the MAC layer of LoRaWAN, by mapping the DIFS and the backoff windows of IEEE 802.11 and IEEE 802.15.4 to consecutive CADs [22]. To and Duda evaluated CSMA with backoff periods in LoRaWAN, using simulation and taking also into account the impact of capture effect on the frame drop rate [23]. Kouvelas *et al.* introduced *p*-CARMA, which uses CAD as CS-mechanism to increase the scalability. In *p*-CARMA, each device adapts its persistence *p* of transmission in a distributed manner based on the results of CAD in its vicinity [14]. Gamage *et al.* designed LMAC [15], a series of CSMA-based MAC protocols of increasing complexity; spanning from LMAC-1 that translates DIFS over several CADs, to LMAC-3 wherein the gateway broadcasts traffic information to assist devices in channel hopping. Beltramelli *et al.* derived an analytical model for the performance of LoRaWAN under (slotted) Aloha and *np*-CSMA regarding throughput, coverage, and consumption, accounting CE in their analysis [24].

*np*-CECADA uses the realistic assessment of CE to adaptively set the transmission power in order to reduce network interference and energy consumption. To the best of our knowledge, *np*-CECADA is the first MAC protocol for LoRaWAN incorporating directly in its way of operation – deciding on whether transmissions will take place – the on-field characterization of CE. Furthermore, *np*-CECADA is the first protocol wherein devices adaptively set their backoff window, after assessing the traffic in their vicinity using CAD, in order to increase the success rate.

### III. DESIGN OF *np*-CECADA

We use both Collisions and CE to our advantage. Former assists in estimating hidden terminals as *np*-CECADA picks probabilistically the “proper” time instance for each device to transmit. Latter helps adapting the transmission power in order to further reducing power consumption and collisions due to hidden terminals. The implementation of *np*-CECADA should not require any changes in the current LoRaMAC protocol and in the gateway. The following LoRa-constraints are met:

**Distributed protocol.** Devices decide independently when to

transmit in an unslotted manner. The gateway may only assist indirectly but never dictate transmission times.

**Low complexity MAC.** Algorithm complexity should be low since LoRa-devices are of low computational capability.

**Minimal changes in devices.** The current frame structure and operating principles of LoRaWAN should not be changed except deciding when to transmit [5].

Along with the above, we add the following design goals to increase the performance of LoRaWAN:

**Increase in capacity.** Referring to throughput per coverage area, by increasing channel use for received frames, capacity is increased as higher traffic loads can be accommodated.

**Scalability.** It refers to collision avoidance which improves PRR and thus increases the effectiveness of communication, i.e., for the same PRR more devices can be accommodated.

**Minimize energy overheads.** *np*-CECADA function must not increase energy consumption.

#### A. Characterization of CE

To leverage CE in the MAC layer of LoRaWAN, its behavior needs to be evaluated first. Bor *et al.* showed that one of the two overlapping transmissions can be correctly received if critical symbols of its frame were not interfered [7]. To study the CE we performed extensive experiments to induce collisions and evaluate the differences in transmission power and delay offset with 0.25 dBm and 5 ms granularity, respectively. Frames of 20 B were transmitted on SF7, SF10, and SF12 using 2 and 3 transmitting devices. We used SX1261 LoRa chipsets operating at 868.1 MHz. The transmitters and receiver were located at LoS and distance of 100 m to avoid antenna perturbations, the bandwidth was 125 kHz, and the CR was 4/5. One extra LoRa-device was used as a moderator which was arranging the delay offsets among the interferers through beacons. During the experiments there was external interference from both non-LoRa and LoRa antennas.

**Effect of Power Difference on CE.** Fig. 3 shows the PRR when two devices –being in the same fading environment– transmit simultaneously with different power. Device A (blue-Tx A) transmits with 7 dBm while device B (red-Tx B) sweeps between 0-14 dBm. We list our observations below.

**Observation #1.** In SF7 and SF10, a power difference below -1.25 dBm and above 2 – 2.5 dBm guarantees the medium is captured by one of the devices, i.e.,  $PRR \geq 90\%$  in Fig. 3a and Fig. 3b. In SF12, the CE is more evident as transmission power difference increases (Fig. 3c). The mean value of PRRs of the dominating devices is 0.923 and the deviation 0.092.

**Observation #2.** When both devices use high transmission powers, the dominating one needs higher power difference in absolute terms to establish a guaranteed CE. For example, in Fig. 3a when the difference is -1.5 dBm (see on x-axis, Tx A: 7 dBm, Tx B: 5.5 dBm),  $PRR_A = 0.95$ , if the difference is +1.5 dBm (Tx A: 7 dBm, Tx B: 8.5 dBm),  $PRR_B = 0.65$ .

**Observation #3.** As seen in Fig. 3 the number of corrupted frames is increased in SF7, while almost absent in SF12. Since higher SFs utilize longer chirps to establish more robust transmissions, they are less prone to corruption.



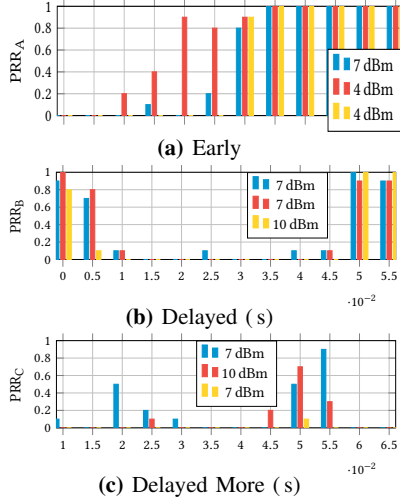


**Fig. 4. PRR based on power difference and delay offset (SF7 and three transmitters).**

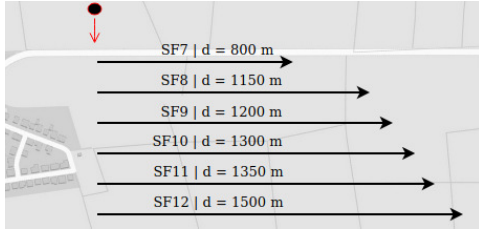


**Fig. 5. Maximum distance for successful CAD per SF.**

#### Delay Offset

The delay offset affects CE more critically than the power difference if the *early* device, i.e., device transmitting first, manages to transmit at least the preamble of its frame without being obstructed. In Fig. 4, the early device A transmits at stable periodicity while the delayed device B transmits with an offset as shown on the x-axis and device C with a larger offset. Each color corresponds to the same experiment with different transmission power per device.

**Observation #4.** As observed, during the preamble period the stronger transmitter has more chances to capture the medium, even if it transmits a few preamble symbols later, e.g., yellow and red color in the first 5 ms of Fig. 4. However, if a device manages to transmit its whole preamble, then the interferers can only corrupt the ongoing transmission, rather than capturing the channel, i.e., after 5 ms. If the delay is longer than frame Time on Air (ToA), transmitter A finishes before interfering with B and C, one of which manages to capture the channel subsequently, after 45 ms.

**Observation #5.** When more than two transmitters are involved, as seen in Fig. 4, the capture effect is mostly determined by the interaction between the two earliest transmissions, i.e., between Fig. 4a and Fig. 4b, regardless of the density of the deployment.

**Observation #6.** When more than half of the payload is transmitted without interference, the early node has an even higher chance to capture the channel, i.e.,  $PRR > 0.8$ .

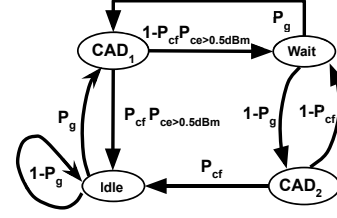


**Fig. 6. Markov model of  $np$ -CECADA for a single device.**

#### B. Characterization of CAD detection

Channel Activity Detection (CAD) can efficiently detect the presence of parts of LoRa-frames on the channel so that frames can be transmitted avoiding collisions [12]. Since we exploit CAD in  $np$ -CECADA to reduce collisions, we must characterize the performance of CAD before employing it in our design. We experimented in Line of Sight (LoS) environment where there are no other LoRa deployments. SX1261 LoRa chipsets are used with six devices configured as stationary receivers on continuous CAD (SF7-SF12) and another device as a mobile transmitter. Although in LoS, we place the receiving devices at a height of 2 m and the transmitter at 1.6 m, introducing corrupting phenomena of multipath propagation and scattering that are observed in long-range transmissions in smart cities. CAD measurements are taken per 50 m, using 2 CAD-symbols for SF7-8 and 4 CAD-symbols for SF9-12. Frames of 20 B are transmitted with 14 dBm. The values of operating frequency, CR, and bandwidth remain the same for all the CE experiments.

**Observation #7.** The CAD performance decreases as distance increases between transmitters and receivers, as seen in Fig. 5.

#### C. $np$ -CECADA

Markov model in Fig. 6 provides the complete picture of  $np$ -CECADA along with transition probabilities that govern every action of a LoRa-device. When a frame is generated with a probability  $P_g$  the device goes to  $CAD_1$  state from Idle and senses the channel. If the channel is free (with  $P_{cf}$ ), the device calculates its chances to capture the channel against the interference from hidden devices. The information on interference (in turn hidden devices) is communicated to the device from the gateway once in a while with broadcast message (see Sec. III-C3). If the device finds that its frame will reach the gateway with RSSI at least 0.5 dBm higher than the interferers (with  $P_{ce} > 0.5dBm$ ), it transmits, adapts its transmission power for future transmissions, and then returns to Idle state. The choice of 0.5 dBm is substantiated in subsection III-C2. On the other hand, if the channel is busy (i.e.,  $1 - P_{cf}$ ), or if the device finds its transmission power is less than the interferers even when channel is free (with  $P_{cf}(1 - P_{ce} > 0.5dBm)$ ), it backs off. The backoff time covers at least one ToA and is based on the probability of CE and local information of traffic (see Sec. III-C2). The computation of the backoff is in subsection III-C4. At the end of backoff time the device executes the second CAD ( $CAD_2$ ). If the channel is free, with  $P_{cf}$ , the device transmits and returns to Idle state, otherwise it again adapts its backoff value and returns to the Wait state and repeats  $CAD_2$ . While in Wait state, if a new

frame arrives, with  $P_g$ , the current one is dropped and repeats the above procedure for the new frame (see Algorithm. 1)

1) **Network Bootstrapping:** In the initial phase of the operation of  $np$ -CECADA, each device transmits with the maximum allowed power (e.g., 14 dBm in Europe). When a device joins the LoRaWAN, in the device-acceptance message the gateway informs the device about the observed pathloss exponent and the distance. Having this information, and knowing its own transmission power, a device can estimate the RSSI of its frames when they reach the gateway. An **observation window** is defined, accounting the maximum periodicity that a LoRa-device can have, assume  $T$  minutes. Then  $T$  is split into slots of predetermined granularity (here  $T=60$  and slots of 5 min). The network server averages the RSSI-values of the correctly received frames per 5 min for  $T$  and shares the values with the gateway. Then, the gateway broadcasts this information at the end of the observation window. Devices compare this “per slot information of interference” to the RSSI of their own frames at the gateways and thus estimate their probability of capturing the channel per gateway per slot. This mechanism repeats when new devices join and periodically.

2) **Initial backoff mechanism:** Whenever a device senses the channel free in  $CAD_1$  state, it estimates the RSSI of its frame at the gateway using the information received from the gateway. Our extensive on-field CE evaluation showed that the probability of successful reception is more than 50% if RSSI

of the received frame is 0.5 dBm higher than the interference – across all SFs. Since the channel conditions and the traffic may change, devices can only take soft decision to transmit (in this step) thus we fix 50% probability. Knowing the average RSSI of interference in the specific time slot (note that we take average RSSI of only the successful frames estimates interference on higher side), the device transmits only if its frame is estimated to have at least 0.5 dBm higher RSSI. Otherwise, it backs off depending on its estimated probability of CE based on our on-field experiments, see line 9 of Alg. 1.

3) **Adaptive transmission power:** Each device also collects the statistics of the number of times it backed off or transmitted during an observation period (e.g., 1 hour). After finding the channel free in  $CAD_1$  state if a device transmitted directly all the times or most of the times, it decreases its transmission power by 0.5 dBm or 0.25 dBm, respectively. By gradually reducing their transmission power over time, devices reach a stage where their frames are received only by one or two gateways, the ones with better channel thus saving energy. The changes in transmission power affect the stability of the whole LoRaWAN which needs to re-converge as the sectors of (non)-hidden devices are updated and the probabilities of finding the channel free/occupied are changed (see Sec. III-C4).

4) **Adaptive Backoff:** In case of deployment of  $N$  LoRa-devices with no hidden devices, and assuming equal frame sizes, a naive Binary Exponential Backoff (BEB) algorithm can maximize the medium access. Assuming a uniform distribution of backoff times, the expected backoff time for each device after a certain number of collisions will converge to the average [13]. However, in LoRa networks there are many hidden devices and CAD cannot guarantee reliable channel sensing of non-hidden devices. Further, not all devices have the same periodicity in transmitting or the same number of neighbors in their vicinity. Therefore, an adaptive method of choosing backoff times will fit the needs of each device. The Markov chain of Fig. 6 is positive, recurrent, and irreducible having the following transition matrix:

	Idle	Wait	$CAD_1$	$CAD_2$
Idle	$1 - P_g$	0	$P_g$	0
Wait	0	0	$P_g$	$1 - P_g$
$CAD_1$	$P_{cf}P_{ce>0.5dBm}$	$1 - P_{cf}P_{ce>0.5dBm}$	0	0
$CAD_2$	$P_{cf}$	$1 - P_{cf}$	0	0

A device can either be in a sensing state ( $CAD_1$  and  $CAD_2$ ) or in non sensing state (Idle and Wait).  $P_g$  is not affected by MAC. Further, the probability of estimating frames being received with more than 0.5 dBm than interference,  $P_{ce>0.5dBm}$ , depends on the fading environment, the interferers, and the network topology. Therefore, the device being in sensing state is affected majorly by the probability of finding the channel free,  $P_{cf}$ . According to Fig. 6, high  $P_{cf}$  leads to more transmissions and thus less time backing off (Wait state). However, frequent transmissions of one device reduce the probability of finding the channel free for other devices; they in turn spend more time backing-off. This leads its neighbors' neighbors to be more aggressive since they find the medium free more

---

**Algorithm 1:** Pseudo code of  $np$ -CECADA

---

```

/* Initial State: Idle */
Result: Transmit or drop the frame
1 Perform  $CAD_1$ 
2 if channel found free then
3   if Tx power of frame is found to be at least 0.5 dBm stronger than
   estimated interference then
4     Transmit the frame
5     Adapt transmission power
6     Return to Idle
7   else
8      $T_xmax = \tau + ToA + (1.0 - P_{ce})ToA$ ; //  $\tau$  is the current time,
//  $(1 - P_{ce})$  the complementary of probability to
capture the channel
9     Backoff with  $backoff\_time \in [\tau + ToA, T_xmax]$ 
10  end
11 else
12   $T_xmax = \tau + ToA + D_B$ ; //  $D_B$ , the backoff delay, depends on local
// traffic found from Eq. 1
13  Backoff with  $backoff\_time \in [\tau + ToA, T_xmax]$ 
14 end
15 while  $backoff\_time > 0$  do
16   sleep ( $backoff\_time$ )
17   if new frame has arrived then
18     Drop current frame
19     break /* go to line 1 */
20   else
21     Perform  $CAD_2$ 
22     if channel found occupied then
23        $T_xmax = \tau + D_B$ 
24       Backoff with  $backoff\_time \in (\tau, T_xmax]$ 
25     else
26       Transmit the frame
27       Return to Idle
28       break
29     end
30  end
31 end

```

---

often. From the above, it is obvious that we are led to a circular argument, as the network dynamics, i.e., transmission power and probabilities of transmission, dynamic traffic load, number of hidden devices do not allow an optimal solution regarding the backoff values. This Markov model cannot represent analytically the inter-dependency among devices in a LoRaWAN, and must be generalized to involve  $N$  devices. However, the complexity of such a model is immense as it should involve  $O(4^N)$  states. Thus, we utilize heuristics to adapt the backoff value.

**Heuristic Approach.** The backoff value,  $B$ , of a device is adapted based on,

$$B = 2^{(1-p) \log_2 N} (1 + Q). \quad (1)$$

$N$ , the number of devices, changes when devices join/leave the network, and this information is piggybacked on Adaptive Data Rate (ADR) messages by the gateway;  $p$  persistence probability is found using the local information of each device regarding the traffic in its vicinity.  $Q$  is the percentage of collided frames (in each observation window), representing the traffic seen by the gateway. In sequel we explain how to find  $p$  and  $Q$ .

**Persistence probability  $p$  via local information.**  $p$  is estimated locally by each device while performing CAD.  $p$  is computed as,

$$p = \frac{\bar{d} - d_l}{(d_h - d_l)} \frac{f}{(b + f)}, \quad (2)$$

where  $\bar{d}$ ,  $d_l$ , and  $d_h$  represent the mean, the lowest, and the highest value of delay the frames experience from the moment they are generated till they are transmitted or dropped.  $\bar{d}$  indirectly represents the traffic created by the non-hidden devices and the probability of each device capturing the channel.  $f$  and  $b$  are the number of times channel was sensed free or busy/occupied in CAD<sub>1</sub>.  $f/(b + f)$  denotes the probability to find the channel free on the first sensing, indicating a relatively low/high traffic in the vicinity. The values of  $p$  are initiated per device the moment that the device performs its first backoff and  $p \in [1/N, 1]$ . The lower bound of  $1/N$  offers each device, the minimum chance of attempting to transmit, since as  $p$  decreases the value of backoff,  $B$ , increases exponentially. As observed by Eq. 2 the persistence probability  $p$ , which determines the backoff depends on values that change dynamically. For example, any sudden event causing more frequent reports by some devices affects their neighbors by (i) increasing their  $b$  values since they find the channel occupied more often and (ii) increasing their  $\bar{d}$  values, since the mean delay of their frames from generation till transmission is increased.

**Ratio of collided frames  $Q$ .**  $Q_i$  represents the point of view of the network server regarding the frames of each device  $i$  given by,  $Q_i = C_i / (C_i + S_i)$ , where  $C_i$  number of collided/dropped frames, and  $S_i$  the successfully transmitted frames. The  $Q_i$  is computed by the network server between two ADR messages, using device ID and sequence number of frames (to find lost frames).  $Q_i$  values are clustered into three groups: low, medium, high loss ratio. They are put in the ADR messages and multicasted to the corresponding devices.

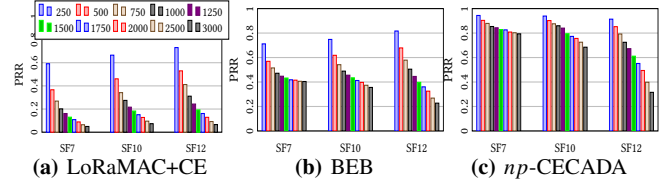


Fig. 7. Mean PRR for increasing number of devices.

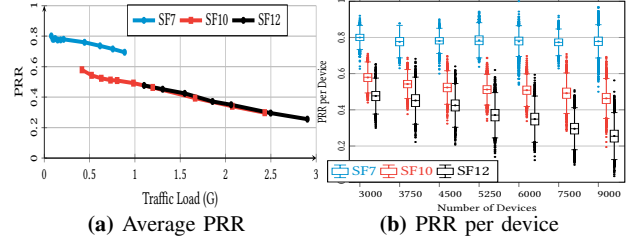


Fig. 8. PRR for np-CECADA with three gateways.

#### IV. SIMULATION-BASED EVALUATION

##### A. Simulation Parameters

Building on the existing simulation code of Magrin *et al.* [4] for vanilla-LoRaWAN in *ns-3*, we designed all the modules and classes required for the application of np-CECADA. Further, we adopted our observations from the on-field experiments on CE and CAD into parameters of LoRa PHY layer (cf. Sec. III-A and Sec. III-B). We simulate scenarios that include up to three gateways and up to 9000 stationary devices positioned around the gateways. The devices transmit frames of 20 B which also include 2 B for ID and sequence number. The configuration settings used for the simulation are similar to the on-field experiments. Initial transmission power –before the employment of power adaptation algorithm– is 14 dBm. Further, the bandwidth of 125 kHz at the frequency of 868.1 MHz is used for transmission. The metrics used to evaluate the performance of np-CECADA are the following:

**Packet Reception Ratio (PRR).** It is the ratio between successfully received frames and transmitted frames.

**Energy consumption.** The total energy consumed per device for transmitting, receiving, performing CAD, and we are interested in energy per successful transmission.

**Channel utilization.** Refers to the normalized time the channel was occupied by correctly received frames over offered traffic  $G$ , which refers to the normalized generated traffic. High values indicate a proper adaptation of the backoff time to handle the increase in traffic, and thus show improved capacity for the LoRa network.

**Fairness in Service.** We define fairness by evaluating the convergence of the values of PRR per device, i.e., equal chance for every device to transmit when the channel is clear.

np-CECADA is evaluated and compared with: (a) vanilla LoRaMAC; (b) Binary Exponential Backoff (BEB); (c) p-CARMA [14]; (d) LMAC [15]. In the graphs we specify “LoRaMAC+CE” for case (a) to differentiate this work from other simulation-works since we incorporated CE to make decisions on the successful frame reception. The case of BEB refers to MAC that uses CAD for CS and uses classical binary exponential backoffs when channel is busy [13]. We



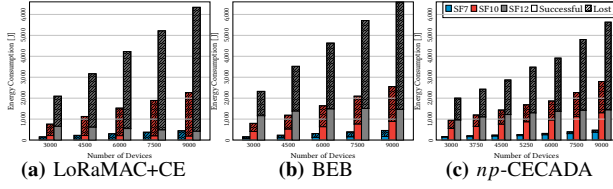


Fig. 9. Energy consumed for successfully received and lost frames for three gateways.

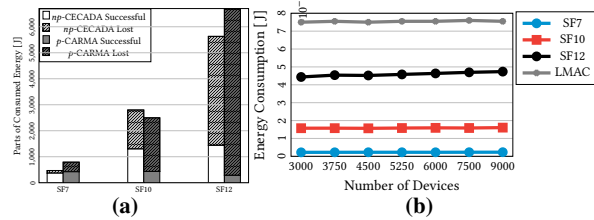


Fig. 10. (a) Comparison of *np*-CECADA with *p*-CARMA and LMAC[15]. Energy consumption for successfully received and lost frames versus *p*-CARMA for 3000 devices per gateway; (b) Energy consumption per frame versus LMAC[15].

simulated 5 hours per case and repeated 30 times to achieve confidence levels of at least 97.5%. Regarding *np*-CECADA, we simulated 15 hours in each run and considered the last 5 hours to find statistically stable results since we have built adaptation in *np*-CECADA. We highlight only the results for SF7, SF10, SF12, as the rest of SFs behave similarly.

### B. Simulation Results

**Packet Reception Ratio.** Fig. 7 presents the performance of the protocols we simulated in terms of PRR for a single gateway. The improvement due to *np*-CECADA compared to LoRaMAC is manifold, specifically from  $16.03\times$  (SF7), to  $9.30\times$  (SF10), to  $4.78\times$  (SF12) when 3000 LoRa-devices are deployed. Further, although BEB achieves higher PRR than LoRaMAC, it is also outperformed by *np*-CECADA by 1.96, 1.92, and 1.39 times, respectively. The gain in scalability is obvious considering the number of devices served for the same PRR. For PRR of 60%, *np*-CECADA serves more than  $12\times$  than LoRaMAC in SF7.

Fig. 8a presents the PRR-performance for three gateways and 1000-15000 devices per gateway. This corresponds to different traffic loads in the x-axis because frames of higher SFs incur more ToA. As observed, the presence of multiple gateways and many thousands of devices did not deteriorate the performance of *np*-CECADA. In specific, the PRR stabilizes between 70-80% in SF7, 30-60% in SF10, and 25-50% in SF12. Compared to *p*-CARMA using 9000 devices, i.e., the maximum for which *p*-CARMA is evaluated, *np*-CECADA outperforms it by  $1.5\times$  to  $5.13\times$  depending on the SF. Note that 9000 devices create a traffic load,  $G$ , of 0.21 in SF7 to 2.9 in SF12. For the same number of devices, vanilla-LoRaMAC is outperformed by  $3.87\times$  to  $15.74\times$  depending on the SF.

The difference between sensing range and transmission range for devices in SF12 is higher, compared to SF10 [25]. Thus we have more hidden terminals on an average in SF12. However, SF12 devices transmit less frames to produce the same traffic (due to higher ToA), thus having less simultaneous

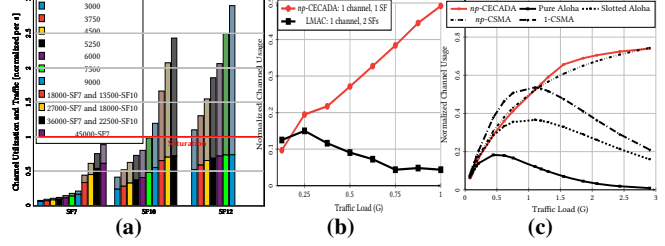


Fig. 11. (a) Normalized channel utilization (vivid colours) and incoming traffic (faded colours) for *np*-CECADA with three gateways; (b) Normalized channel utilization for *np*-CECADA and LMAC; (c) Throughput for *np*-CECADA and four main contention MAC schemes[8].

transmissions. Therefore, they present similar PRR under the same traffic values. In SF7, due to very close distance between devices, hidden terminals on an average are much less than SF10. Therefore, although in SF7 more frames are transmitted for the same traffic load, CAD avoids majority of collisions.

**Fairness.** As seen in Fig. 8b, the deviation of PRR is minimal. Box-plots infer that half of the devices in each case deviate utmost 0.025 from their mean; while, generally, the deviation-from-mean is less than 0.1. The outliers are merely up to 3.3%. *np*-CECADA allows equal chances for devices to access the medium.

**Energy Consumption.** As observed in Fig. 9, regulating transmission power and avoiding transmissions that would collide saves energy. Especially in SF12, where the ToA of each transmission is relatively longer thus consumes more energy. However, *np*-CECADA consumes 30% less than LoRaMAC. In SF7 where less energy is needed per transmission, all protocols consume around the same energy. This is because CAD affects the overall consumption more drastically. Let us observe how much of this energy is useful (i.e., leading to successful transmission). As seen in Fig. 9a, devices in LoRaMAC waste almost all their energy for transmissions that collide, especially at low SFs. The backoff policy employed in BEB offers better performance, but still, more than half of the total energy goes for nothing in all cases, see Fig. 9b. However, *np*-CECADA makes smart usage of the energy, even in cases of many areas of hidden devices like SF12. In particular, *np*-CECADA uses 77.83%, 46.30%, and 25.49% energy corresponding to SF7, SF10, and SF12 for successful transmissions, while 8.06% and 37.01% are the highest that LoRaMAC and BEB can achieve, respectively. Even in the case of the lowest traffic, for 3000 devices in total and in SF7, *np*-CECADA uses 80.1% of its consumed energy for successful transmissions. Contrarily, LoRaMAC and BEB utilize 21% and 48.6%, respectively, while their total consumption is almost equal that of *np*-CECADA. As observed in Fig. 10a, for 3000 devices per gateway only up to 53.17% of the total energy of *p*-CARMA is spent on successful transmissions in SF7. Even in this case of low traffic,  $G=0.21$ , *p*-CARMA is outperformed by  $1.5\times$  by *np*-CECADA. Further, as seen in Fig. 10b for the same payload LMAC consumes around 75 mJ per frame while *np*-CECADA consumes at most 47 mJ.

**Channel utilization.** As observed in Fig. 11a, *np*-CECADA boosts channel utilization due to better distribution of trans-

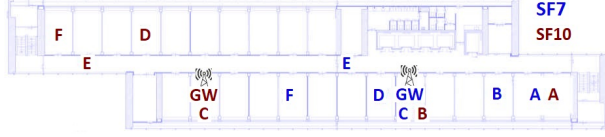


Fig. 12. Thirty devices in six groups. Floor-plan with group-positions according to their SF. Gateway positioned with group C. Group E is one floor below the other groups.

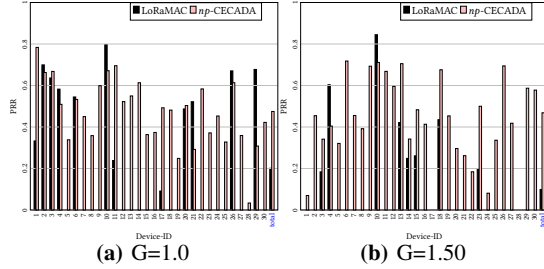


Fig. 13. PRR per device: *np*-CECADA versus LoRaMAC and in total for different traffic loads at SF7.

missions over time. The increase in channel utilization (see vivid colors) versus normalized traffic,  $G$ , (see faint colors) exemplifies the scalability potential of *np*-CECADA, especially for SF7. This ratio stays between 80%-69% for  $G \in [0.08, 0.89]$  in SF7, 57.9%-29.7% for  $G \in [0.58, 2.43]$  in SF10, and 47.6%-25.5% for  $G \in [1.1, 2.9]$  in SF12. Notice that useful channel utilization stays stable in SF10 and SF12 even when the channel is well beyond saturation (red line); namely, utilization of 0.74 is achieved for both SFs even up to normalized traffic of 2.43 and 2.9 for SF10 and SF12, respectively. This illustrates the potential of adapting transmission time in high traffic conditions. In Fig. 11b, *np*-CECADA is compared with LMAC on channel utilization basis for increasing levels of traffic. Since LMAC uses simultaneously 16 different combinations among 8 channels and 2 SFs, we downscale per channel. *np*-CECADA outperforms LMAC in any traffic condition. Specifically at  $G = 1$ , *np*-CECADA achieves eleven-fold improvement. The effectiveness in utilizing the medium by *np*-CECADA is highlighted in Fig. 11c, being compared even to the classic *p*-CSMA and *np*-CSMA protocols which use sophisticated feedback mechanisms (ACKs, RTS/CTS) and continuous sensing (*p*-CSMA). As observed, *np*-CECADA outperforms 1-CSMA above  $G=1$ . For  $G<1$ , 1-CSMA presents higher channel usage than *np*-CECADA, but 1-CSMA uses continuous active channel sensing, consuming humongous amounts of energy to operate, and thus is not suitable for LoRa networks. *np*-CECADA behaves similarly to the classic *np*-CSMA while having minimum feedback from the gateway, with an inferior sensing mechanism (CAD), and consuming minimum energy.

## V. PRACTICAL EVALUATION

It is hard to test *np*-CECADA in commercial LoRa deployments thus we created a simple testbed involving 30

TABLE I

Groups of non-hidden devices for each group

Group	Non-hidden	Group	Non-hidden	Group	Non-hidden
A	B, C	B	A, C, D	C and GW	A, B, D, E, F
D	B, C, E, F	E	C, D, F	F	C, D, E

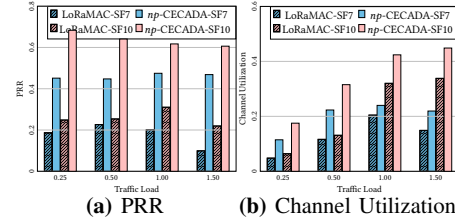
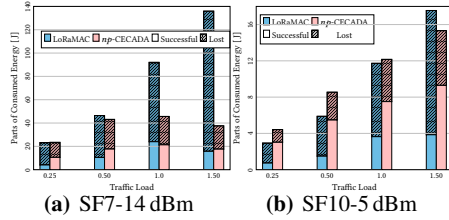


Fig. 14. PRR and channel utilization for *np*-CECADA and LoRaMAC for different traffic loads and SFs.

LoRa SX1261 *class A* devices (with STM32 Nucleo-F446RE MCU) and one gateway in indoors emulating a LoRaWAN without interference from commercial operations. As shown in Fig. 12 the 30 devices are clustered into six groups of five devices deployed on two floors in our building. We first fixed the gateway and then we extensively measured the RSSI and successful reception of frames when transmitted from different locations. Then the locations of groups are carefully planned to mimic LoRaWAN with hidden and non-hidden terminals for both SF7 and SF10. Each group can see only a subset of other groups, e.g., group C devices can see all others and group A devices see only the groups B & C (See Table I). The indoor environment offers higher fading because of walls hence we observed higher signal attenuation. This setup mimicked an open-field LoRaWAN with devices positioned in large distances also involving hidden devices. In SF10, initial transmission power is 5 dBm to achieve the same pattern of hidden devices as that of SF7 where 14 dBm was used (See Table I). To emulate large numbers of devices we increased the duty cycle (above 1%) and frame sizes so that the offered load,  $G$ , is close to what is seen by a gateway in practice to test scalability. We evaluated one hour of operation under *np*-CECADA and vanilla LoRaMAC for  $G \in [0.25, 0.5, 1.0, 1.5]$ . Multiple experiments were done with frames of 200 B and 40 B for SF7 and SF10, correspondingly. The rest of the parameters remain unchanged. The PRR of each device is presented in Fig. 13. For brevity, we present the results for SF7 and high traffic loads, as the ones for SF10 are analogous. As observed, the devices which perform better when *np*-CECADA is used vary from 24 to 28 out of 30, depending on the traffic. More importantly, *np*-CECADA manages to distribute the transmissions much more fairly among the devices as shown by the lesser variations in PRR. On the contrary, the vast majority of devices have 0% PRR if LoRaMAC is used. Few devices (between 2 and 6) have high individual PRR-values in LoRaMAC because of their positions (fading and distance from the gateway). Therefore, they dominate the channel at the expense of all the others and of the overall PRR since simultaneous transmissions cannot be evaded. The overall PRR for SF7 and SF10 is presented in Fig. 14a. *np*-CECADA outperforms LoRaMAC by  $2\times$  to  $4.7\times$  in SF7 and by  $1.5\times$  to  $2.76\times$  in SF10 for  $G=[0.25, 0.5, 1.0, 1.5]$ . Regarding channel utilization (see Fig. 14b), in SF7 *np*-CECADA manages more than 20% even in heavy traffic of  $G=1.50$  while LoRaMAC shows signs of collapse since its channel utilization decreases drastically. In SF10 for the



**Fig. 15. Energy consumption for *np*-CECADA and LoRaMAC for different traffic loads. The parts of energy spent for successful and failed frames are depicted.**

same traffic *np*-CECADA has 0.45 utilization which is  $\approx 30\%$  more compared to 0.33 for LoRaMAC. Note that higher than theoretical utilization of 0.18 for LoRaMAC is because of CE. In SF7 the transmission power is 14 dBm; LoRaMAC consumes up to  $3.6\times$  more energy than *np*-CECADA for  $G=1.50$ , since the transmissions are not regulated by the MAC (see Fig. 15a). Only 11.6% of the energy is used for successful transmissions, contrary to *np*-CECADA where it is up to 46.8%. In SF10 the overall consumption is heavily decreased for both the protocols since the transmission power is decreased to 5 dBm (see y-axis of Fig. 15b). The difference in consumption between them is smaller because the cost of transmissions is decreased, while the cost of CAD remains the same. Nevertheless, 60-68% of energy in *np*-CECADA is used for successful transmissions while in LoRaMAC it is 31%.

## VI. CONCLUSIONS

We proposed a novel algorithm, *np*-CECADA, to address the PRR and scalability of LoRaWAN without changing the protocol and Gateway code by adapting the backoff duration at each device independently and distributively using the imperfect CAD that senses the channel. *np*-CECADA leverages the capture effect phenomenon to reduce the transmission power of each device without compromising PRR, leading to less interference in the network. We implemented *np*-CECADA on a small testbed and for scalability studies we developed *ns-3* modules. *np*-CECADA improves PRR by 4 to 16 times depending on the SF compared to LoRaMAC in a 3 gateways network and scales up to 9000 devices and outperforms *p*-CARMA by 1.5 to 5.13 times. Further, the cost per transmission with *np*-CECADA varies between 2-47 mJ, while LMAC consumes 75 mJ per frame. Furthermore, the adaptive characteristic of *np*-CECADA allows PRR per device to converge guaranteeing fairness in channel access. In our experiments for  $G=1.5$ , the average PRR was 47% and 61% for SF7 and SF10, respectively; while with LoRaMAC majority devices did not even manage a single successful transmission. *np*-CECADA offers high levels of throughput even in heavily saturated networks, i.e.,  $G>1.0$ , resembling the performance of the classic *np*-CSMA but with very rare feedback from gateways and without continuous sensing. Finally, *np*-CECADA can be directly and progressively implemented in legacy LoRaWAN without deviating from the existing standard.

## VII. ACKNOWLEDGEMENT

InSecTT has received funding from the ECSEL Joint Undertaking (JU) under grant agreement No 876038. The JU

receives support from the European Union's Horizon 2020 research and innovation programme and Austria, Sweden, Spain, Italy, France, Portugal, Ireland, Finland, Slovenia, Poland, Netherlands, Turkey. The document reflects the author's view only and the Commission is not responsible for any use that may be made of the information it contains.

## REFERENCES

- [1] M. Centenaro, L. Vangelista, A. Zanella, and M. Zorzi, "Long-range communications in unlicensed bands: the rising stars in the IoT and smart city scenarios," *IEEE Wireless Communications*, vol. 23, 2016.
- [2] J. Petäjäjärvi, K. Mikhaylov, M. Pettissalo, J. Janhunen, and J. Linatti, "Performance of a low-power wide-area network based on LoRa technology: Doppler robustness, scalability, and coverage," *IJDSN*, 2017.
- [3] J. C. Liando, A. Gamage, A. W. Tengourti, and M. Li, "Known and Unknown Facts of LoRa: Experiences from a Large-Scale Measurement Study," *ACM Trans. Sen. Netw.*, vol. 15, no. 2, feb 2019.
- [4] D. Magrin, M. Capuzzo, and A. Zanella, "A Thorough Study of LoRaWAN Performance Under Different Parameter Settings," *IEEE IoT-J*, vol. 7, no. 1, pp. 116–127, 2020.
- [5] LoRa™ Alliance, "LoRaWAN® Specification v1.1," <https://lorawan-alliance.org>, [Online; accessed: 2020-10-10].
- [6] B. Ghena, J. Adkins, L. Shangguan, K. Jamieson, P. Levis, and P. Dutta, "Challenge: Unlicensed LPWANs Are Not Yet the Path to Ubiquitous Connectivity," in *ACM MobiCom*, 2019.
- [7] M. C. Bor, U. Roedig, T. Voigt, and J. M. Alonso, "Do LoRa Low-Power Wide-Area Networks Scale?" in *ACM MSWM*, 2016, pp. 59–67.
- [8] L. Kleinrock and F. Tobagi, "Packet Switching in Radio Channels: Part I - Carrier Sense Multiple-Access Modes and Their Throughput-Delay Characteristics," *IEEE TCOM*, vol. 23, no. 12, pp. 1400–1416, Dec 1975.
- [9] J. Lee, W. Kim, S.-J. Lee, D. Jo, J. Ryu, T. Kwon, and Y. Choi, "An Experimental Study on the Capture Effect in 802.11a Networks," in *ACM WinTECH '07*, 2007, p. 19–26.
- [10] R. Fernandes, R. Oliveira, M. Luís, and S. Sargento, "On the Real Capacity of LoRa Networks: The Impact of Non-Destructive Communications," *IEEE Communications Letters*, vol. 23, 2019.
- [11] P. Marcellis, N. Kouvelas, V. S. Rao, and V. Prasad, "DaRe: Data Recovery through Application Layer Coding for LoRaWAN," *IEEE Transactions on Mobile Computing*, pp. 1–1, 2020.
- [12] Semtech, "Application Note: SX126x CAD Performance Evaluation," <https://semtech.my.salesforce.com>, [Online; accessed 2020-10-8].
- [13] G. Bianchi, "Performance analysis of the IEEE 802.11 distributed coordination function," *IEEE JSAC*, vol. 18, no. 3, pp. 535–547, 2000.
- [14] N. Kouvelas, V. S. Rao, R. V. Prasad, G. Tawde, and K. Langendoen, "P-CARMA: Politely Scaling LoRaWAN," in *ACM EWSN*, 2020.
- [15] A. Gamage, J. C. Liando, C. Gu, R. Tan, and M. Li, "LMAC: Efficient Carrier-Sense Multiple Access for LoRa," in *MobiCom*. ACM, 2020.
- [16] T. Polonelli, D. Brunelli, A. Marzocchi, and L. Benini, "Slotted ALOHA on LoRaWAN-Design, Analysis, and Deployment," *Sensors*, Feb 2019.
- [17] K. Q. Abdelfadeel, D. Zorbas, V. Cionca, and D. Pesch, "FREE—Fine-Grained Scheduling for Reliable and Energy-Efficient Data Collection in LoRaWAN," *IEEE IoT-J*, vol. 7, no. 1, pp. 669–683, 2020.
- [18] Z. Xu, J. Luo, Z. Yin, T. He, and F. Dong, "S-MAC: Achieving High Scalability via Adaptive Scheduling in LPWAN," in *IEEE INFOCOM*.
- [19] D. Zorbas, K. Abdelfadeel, P. Kotzanikolaou, and D. Pesch, "TS-LoRa: Time-slotted LoRaWAN for the Industrial Internet of Things," *Computer Communications*, vol. 153, pp. 1 – 10, 2020.
- [20] B. Reynders, Q. Wang, P. Tuset-Peiro, X. Vilajosana, and S. Pollin, "Improving Reliability and Scalability of LoRaWANs Through Lightweight Scheduling," *IEEE IoT-J*, vol. 5, no. 3, pp. 1830–1842, 2018.
- [21] L. Leonardi, F. Battaglia, and L. Lo Bello, "RT-LoRa: A Medium Access Strategy to Support Real-Time Flows Over LoRa-Based Networks for Industrial IoT Applications," *IEEE IoT-J*, vol. 6, 2019.
- [22] C. Pham, "Investigating and experimenting CSMA channel access mechanisms for LoRa IoT networks," in *IEEE WCNC*, April 2018.
- [23] T. To and A. Duda, "Simulation of LoRa in NS-3: Improving LoRa Performance with CSMA," in *IEEE ICC*, May 2018, pp. 1–7.
- [24] L. Beltramelli, A. Mahmood, P. Österberg, and M. Gidlund, "LoRa beyond aloha: An investigation of alternative random access protocols," *IEEE TH*, vol. 17, no. 5, pp. 3544–3554, 2021.
- [25] C. Pham and M. Ehsan, "Dense Deployment of LoRa Networks: Expectations and Limits of Channel Activity Detection and Capture Effect for Radio Channel Access," *Sensors*, vol. 21, 2021.